Journal of Chemical&Engineering Data

pubs.acs.org/jced
Article

Thermophysical Properties of Mixtures Containing Cholinium L Alaninate and Water, Ethanol, or Propan-1-ol

Pedro Velho Berta N. Estevinho and Eugénia A. Macedo

Cite This: J Chem Eng Data 2024 69 338−347

ABSTRACT: Choline amino acid ionic liquids (CAAILs) provide a greener alternative to classical ionic liquids, such as the ones based on imidazolium cations, since they can be obtained from natural sources with larger biodegradability. Given that most industrial extractions are performed in either aqueous or alcoholic media, the thermophysical characterization of binary mixtures containing these solvents is very important for process design. In this work, the influences of the mole fraction of ionic liquid and of temperature on the thermophysical properties of binary mixtures containing water, ethanol, or propan-1-ol and cholinium L-alaninate ([Ch][Ala]), a well-known CAAIL, were studied. Dynamic viscosity, shear stress, torque (T = 288.15 − 308.15 K), electrical conductivity (T = 298.15 K), and density (T = 293.15, 298.15, 303.15 K) were measured at 0.1 MPa, and the corresponding excess volumes were calculated and fitted to a Redlich−Kister (RK) equation. Moreover, the effect of temperature on density (T = 288.15 − 323.15 K), dynamic viscosity (T = 288.15 − 323.15 K), and refractive index (T = 288.15 − 343.15 K) of the synthesized [Ch][Ala] was also evaluated and compared with literature. Dynamic viscosities of the pure components were determined and fitted using the Vogel−Fulcher−Tammann−Hesse (VFTH) equation.

1. INTRODUCTION

Ionic liquids (ILs) or molten salts have been increasingly studied for application in separation processes in the last two decades due to their high heat capacities, high thermal stability, low volatilities, and nonflammability.[1] Moreover, ILs are liquid over a wide range of temperature,[1,2] which makes them more versatile than other solvents, such as deep eutectic solvents (DESs). The most preponderant examples of successful applications of ILs are the removal of pharmaceuticals from wastewater[3,4] and the elimination of heavy metals from contaminated debris.[5,6] Furthermore, given their generally high conductivity and density, this class of electrolytes is also expected to play a distinguished role in the development of technologies such as batteries and photoelectrical cells.[1,7,8]

In the pharmaceutical industry, a very active search for new solutions is taking place to revolutionize the existing medicines and pharmaceutical formulations and to create new and more effective treatments. Active pharmaceutical ingredient (API)-based ionic liquids (API-ILs) present an exciting new paradigm for the formulation of poorly water-soluble drugs since they can be used to mediate the release of APIs in response to external stimuli, increase bioavailability, and address polymorphism issues, taking advantage of their tunability and well-defined controlled release.[9−11] However, the API-IL strategy presents several challenges which demand deep research before it can be a viable approach to formulate APIs with poor aqueous solubility and replace other more mature techniques such as salt formation, solid dispersion, nanosuspensions, and micellar systems.[11] Ionic liquids are generally difficult materials to work with as they generally exist at room temperature and pressure as viscous oils, making handling, processing, and formulation for different solid applications very problematic.[12] To alleviate this, it has been shown that API-ILs can be combined with other materials such as ionogels or mesoporous silica[9] or immobilized via microencapsulation, forming capsules with small size but vast total interfacial area.[13] Hence, microencapsulation of ionic liquids has been described to be an essential step in the production of, for example, delivery vehicles for chemical compounds[11,12,14,15] and of self-lubricating coatings.[16] Nevertheless, when microencapsulation is not possible, the application of these solvents in processes at industrial scale and in separations involving labile species such as proteins and antioxidants is severely hampered mainly by their high density and significant toxicity. Also, the high cost and poor biodegradability of most ionic liquids created the need for greener processual alternatives.[17]

Special Issue: In Honor of Gabriele Sadowski

Received: April 21, 2023
Accepted: August 2, 2023
Published: August 10, 2023

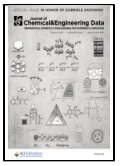

Table 1. List of chemicals used in this work with respective chemical formula, supplier, purity, density at 298.15 K and 0.1 MPa), CAS number, and abbreviation.

chemical	supplier	purity / m [a]	density / kg·m^{-3} exp.	density / kg·m^{-3} lit.	CAS	abbrev.
choline chloride ($C_5H_{14}NOCl$)	VWR Chemicals	> 98.0[b]			67-48-1	[Ch]Cl
cholinium L-alaninate ($C_8H_{20}N_2O_3$)	Synthesized in this work	> 99.0[c]	1125.20[c]	1129.98[39]	1361335-79-6	[Ch][Ala]
L-alanine ($C_3H_7NO_2$)	Merck	> 99.0[b]			302-72-7	Ala
ethanol (CH_3CH_2OH)	Sigma-Aldrich	> 99.0[b]	785.22[c]	784.93[32]	64-17-5	EtOH
potassium hydroxide (KOH)	Merck	> 90.0[b]			1310-58-3	KOH
propan-1-ol ($CH_3CH_2CH_2OH$)	VWR Chemicals	> 99.8[b]	800.05[c]	799.60[32]	71-23-8	PrOH

[a]m refers to mass percentage. [b]Provided by the supplier. [c]Determined in this work. The combined expanded uncertainties (U_c) and relative expanded uncertainties (U_r), for a level of confidence of 95 and a combined coverage factor of 1.96,[40] are $U_r(\rho)$ = 0.001 and $U_c(T)$ = 0.02 K.

To mitigate some of these issues, the choline amino acid ionic liquids (CAAILs or ChAA-ILs), *i.e.*, ionic liquids based on amino acids and choline (essential nutrient), were developed. CAAILs, first synthesized by Moriel *et al.*,[18] combine a quaternary amine as cation (choline) with the carboxylic functional group of amino acids and present lower toxicity and higher biocompatibility compared to the classical ionic liquids, such as the ones based on imidazolium, pyrrolidinium, and pyridinium cations.[19−21] Moreover, CAAILs can be produced in a relatively cheap fashion and taking advantage of natural and easily available resources, given that choline is a B-complex nutrient and that amino acids are the building blocks of proteins, decreasing the environmental impact of solvent synthesis.[17,18] Similarly to API-ILs, CAAILs have also been used to increase the solubility of poorly water-soluble drugs such as lamotrigine,[22] improving the design of crystallization processes and allowing the validation of thermodynamic models.[23] Furthermore, CAAILs have been effectively applied in the partition of biomolecules, such as amino acids,[19] proteins,[24] antioxidants,[25,26] and pigments,[27] in biomass valorization,[21,28] and in carbon dioxide capture[21,29] and are considered outstanding biocompatible media for biocatalytic applications.[30]

In this work, the goal was to assess the influences of the mole fraction of ionic liquid and of temperature on the thermophysical properties of binary mixtures containing water, ethanol or propan-1-ol and cholinium L-alaninate ([Ch][Ala]), a well-known CAAIL. Therefore, dynamic viscosity, shear stress, torque (T = 288.15 − 308.15 K), electrical conductivity (T = 298.15 K), and density (T = 293.15, 298.15, 303.15 K) of the binary mixtures were measured at 0.1 MPa, and the corresponding excess volumes were calculated. Moreover, the effect of temperature on density (T = 288.15 − 323.15 K), dynamic viscosity (T = 288.15 − 323.15 K), and refractive index (T = 288.15 − 343.15 K) of pure [Ch][Ala], at 0.1 MPa, were also delved into. Finally, the degree of dissociation (or ionicity) of the pure CAAIL was estimated using the Walden plot methodology.

2. EXPERIMENTAL SECTION

2.1. Materials. The list of chemicals and their respective supplying companies, purities, Chemical Abstracts Service (CAS) numbers, and abbreviations are in Table 1. No additional purification steps nor pretreatments were carried out for the commercial chemical species. Density, refractive index, and dynamic viscosity of pure water, ethanol, and propan-1-ol were compared with data from the literature,[31−38] as can be seen in Figures S1−S3.

2.2. Equipment and Procedures. The binary mixtures of cholinium L-alaninate ([Ch][Ala]) with water, ethanol, or propan-1-ol were prepared by weighing the constituent components in an ADAM AAA 250L balance with standard measurement uncertainty of 1 × 10^{-4} g and vigorously stirring for 30 min. To minimize solvent evaporation and to avoid moisture capture by the ionic liquid, all samples were prepared in stoppered vials immediately prior to the experimental measurements. Then, liquid densities (ρ) were assessed with an Anton Paar DSA-4500 M digital vibrating tube densimeter with standard measurement uncertainties of 5 × 10^{-5} g·cm^{-3} and 0.01 K. The equipment was calibrated with Millipore quality water and air according to the technical manual. Electrical conductivities (κ) were measured with a Microprocessor conductivity meter EDT RE387TX with relative measurement uncertainties of 0.01, while dynamic viscosities (η) were evaluated with an Anton Paar MCR92 rheometer with a cone−plate geometry (plate diameter of 25 mm, cone angle of 1°, and measuring gap of 0.5 mm) and relative measurement uncertainty of 0.24. Moreover, refractive indices (n_D) were determined with an ABBE refractometer−Optic Ivymen with standard measurement uncertainties of 0.0002 and 0.01 K, while an ultraviolet−visible (UV−vis) Thermo Scientific Varioskan Flash spectrophotometer with standard measurement uncertainty of 1 × 10^{-4} was used to quantify UV−vis absorbance. Finally, a Mettler Toledo C20 Coulometric Karl Fisher titrator, with a standard measurement uncertainty of 5 ppm, was used to estimate water content and a PerkinElmer Spectrum Two FT-IR, with relative measurement uncertainty of 0.0001, was applied to determine the infrared (IR) transmittance spectrum.

2.3. Synthesis of [Ch][Ala]. In the synthesis of cholinium L-alaninate ([Ch][Ala]), the amino acid (L-alanine) was dissolved in 500 mL of ethanol (CH_3CH_2OH) with an excess of potassium hydroxide (KOH) to create the potassium salt of the amino acid, taking inspiration from other works.[18,26] This mixture, with approximate mass percentages of 25 of amino acid and 15 of salt, was stirred for 3 h at 308.15 K and 0.1 MPa in an OvanTherm MultiMix BHM5E thermoregulated bath before adding choline chloride ([Ch]Cl) in stoichiometric proportions. Then, after being stirred for 12 h at the same temperature and pressure, 200 mL of ethanol were added, and the mixture was filtrated under vacuum to remove the white suspension (potassium chloride, KCl) from the solution. The obtained ionic liquid was dried for 72 h at T = 328.15 K and P = 0.1 MPa in an IKA RV10 rotary evaporator to remove ethanol and water. Afterward, the CAAIL was capped, sealed, and stored at ambient pressure and temperature. Its final water content was assessed before use by a

https://doi.org/10.1021/acs.jced.3c00247
J Chem Eng Data 2024 69 338−347

Mettler Toledo C20 Coulometric Karl Fisher Titrator with a standard measurement uncertainty of 5 ppm, and its chemical structure was confirmed by FTIR spectroscopy. The general reaction route for the synthesis of cholinium L-alaninate is shown in Figure 1.

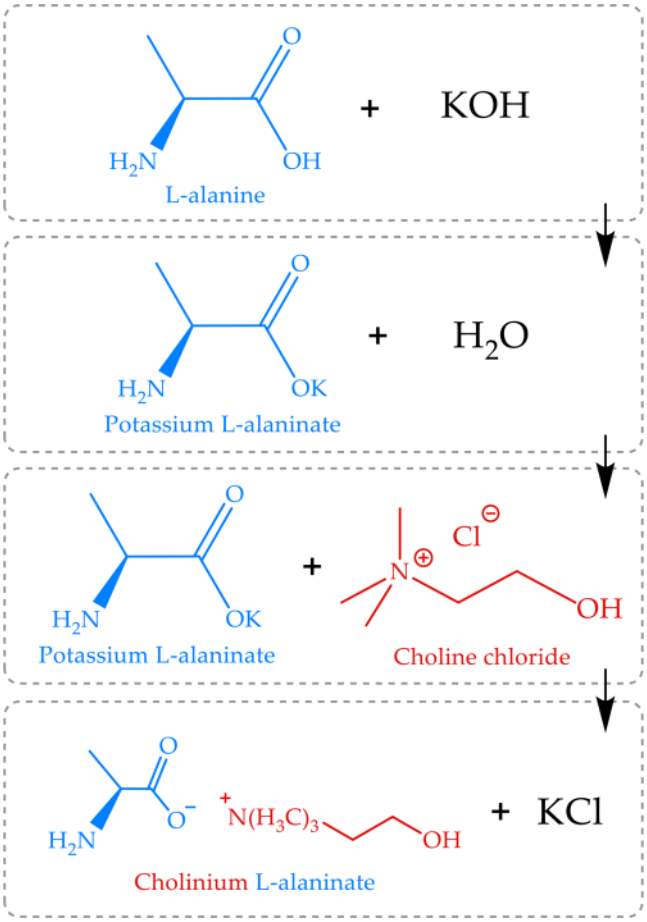

Figure 1. Reaction route for the synthesis of the CAAIL cholinium L-alaninate ([Ch][Ala]).

3. RESULTS AND DISCUSSION

3.1. Pure Ionic Liquid. After having synthesized cholinium L-alaninate ([Ch][Ala]) from choline chloride ([Ch]Cl) and L-alanine, the obtained chemical structure was validated by analyzing its infrared (IR) transmittance spectrum using Fourier-transform infrared (FTIR) spectroscopy, which can be seen in Figure S4. As expected, the most notorious peak was observed at ∼1600 cm^{-1}, corresponding to the asymmetric stretch of the carboxylate group ($RCOO^-$) and agreeing with the available literature.[41,42] At ∼3200 cm^{-1}, a band corresponding to the O−H stretching of the cholinium cation and to the N−H stretching of the L-alaninate cation was found. Moreover, some other peaks were noticed: ∼1475 cm^{-1}, due to the presence of ammonium methyl groups; ∼1355 cm^{-1}, caused by the C−N stretching vibration; ∼1085 cm^{-1}, corresponding to the C−O stretch of choline. Furthermore, the UV−vis absorbance spectrum was also determined and can be found in Figure S5.

Once the chemical structure of the synthesized CAAIL was validated and the water content was assessed by Karl Fisher titration (<100 ppm), the density of cholinium L-alaninate was measured (T = 288.15 − 323.15 K) and compared with the available literature,[41,43] as Figure 2 shows. Even though the

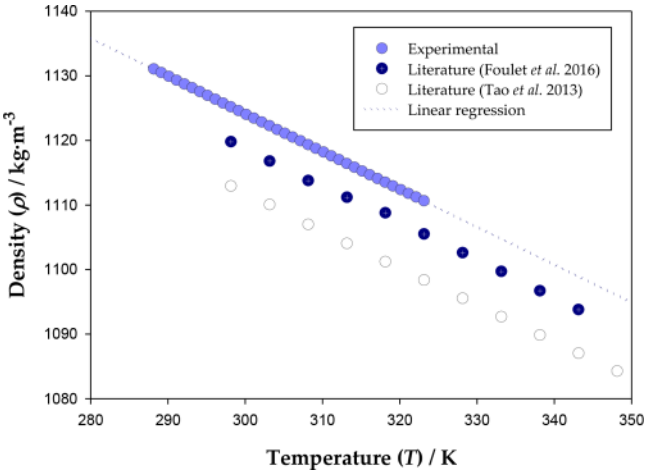

Figure 2. Experimental densities (ρ), at T = 288.15 − 323.15 K and P = 0.1 MPa, for [Ch][Ala] and comparison with the literature.[41,43] The first-degree fitting follows equation ρ ($kg{\cdot}m^{-3}$) = 1299.0 + 1.0840 × 10^{-1} × T (K) with a determination coefficient (R^2) of 1.0000. The combined expanded uncertainties (U_c) and relative expanded uncertainties (U_r), for a level of confidence of 95 and a combined coverage factor of 1.96,[40] are $U_r(\rho)$ = 0.001 and $U_c(T)$ = 0.02 K.

CAAIL synthesized in this work presented a slightly larger density than the ones reported in the literature, which is probably explained by less water contamination, it was considered very similar to the ones in previous works.[39,41,43] The measured data can be found in Table S1.

Refractive indices (n_D) were evaluated for the pure CAAIL, and a linear relation with temperature was found in the studied range (T = 288.15 − 343.15 K), agreeing with previous works.[43] The measured data can be found in Table S1. Dynamic viscosity (η) was also assessed for the pure CAAIL, from T = 288.15 − 323.15 K, and some discrepancy was found with the data published in the literature,[41,43,44] which appears to be quite common[45] given the plethora of existent rheometers. Both thermophysical properties were very well correlated with temperature using polynomial equations, as Figure 3 shows, but, for the case of dynamic viscosity, a more common approach[46,47] is to use the Vogel−Fulcher−Tammann−Hesse (VFTH) equation.[48−50]

The VFTH equation, given by eq 1, is considered the most accurate three-parameter equation for viscosity correlation and is crucial for the treatment of relaxation phenomena in glass-forming and viscous systems.[51,52]

$$\eta \quad \cdot\exp\left(\frac{B}{T - T}\right) \tag{1}$$

where A, B, and T_0 are adjustable parameters and T is temperature.

Even though A and B are considered not to have a particular physical meaning,[53] T_0 started to be referred to as the ideal glass transition temperature since Cohen and Turnbull[54] and Adam and Gibbs[55] developed the free volume theory and the configurational entropy approach, respectively. For the case of [Ch][Ala], the values of the VFTH equation were found to be A = 8.866 Pa·s, B = 30.96 K, and T_0 = 323.3 K with a

https://doi.org/10.1021/acs.jced.3c00247
J Chem Eng Data 2024 69 338−347

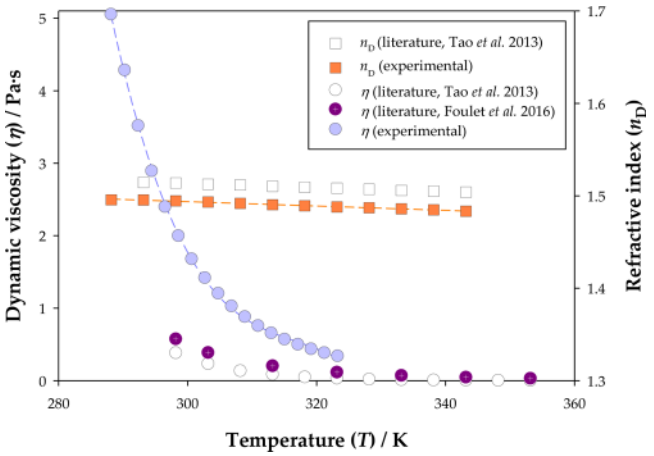

Figure 3. Experimental dynamic viscosities (η), at T = 288.15 − 323.15 K and P = 0.1 MPa, and refractive indices (n_D), at T = 288.15 − 343.15 K and P = 0.1 MPa, for [Ch][Ala] and comparison with the literature.[41,43] The experimental refractive indices follow equation n_D = 1.2990 + 1.0840 × 10^{-4} × T (K) with a determination coefficient (R^2) of 0.9996 and the experimental dynamic viscosities follow equation η (Pa·s) = 5.002 × 10^{-3} − 4.733 × 10^{1} × T (K) + 1.494 × 10^{-1} × T^2 (K) − 1.573 × 10^{-4} × T^3 (K) with a determination coefficient (R^2) of 0.9940. The combined expanded uncertainties (U_c) and relative expanded uncertainties (U_r), for a level of confidence of 95 and a combined coverage factor of 1.96,[40] are $U_c(n_D)$ = 4 × 10^{-4}, $U_r(\eta)$ = 0.24 and $U_c(T)$ = 0.02 K.

determination coefficient (R^2) of 0.8581 and a standard deviation (σ_s) of 0.5 Pa·s.

3.2. Binary Mixtures. Once the components of the binary mixtures were mixed and properly stirred, their densities were evaluated at T = 293.15, 298.15, and 303.15 K and P = 0.1 MPa, as can be observed in Figure 4 and Table S2. Considering the measured solvent densities at 298.15 K (997.1, 758.9, and 800.1 kg·m^{-3} for water, ethanol, and propan-1-ol, respectively), one would expect to observe the highest mixture densities for [Ch][Ala] + water, followed by

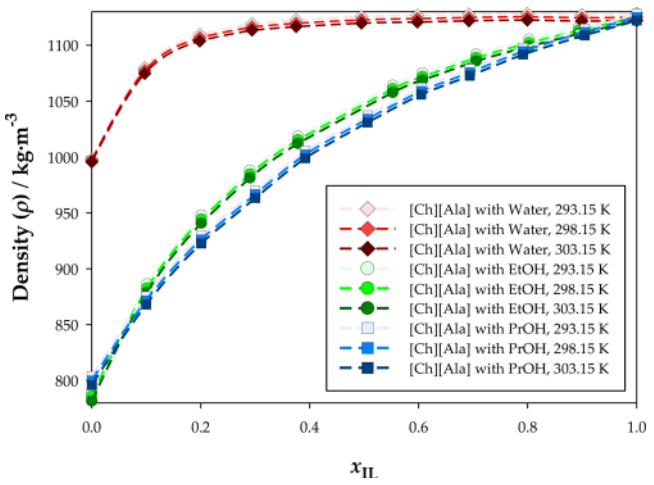

Figure 4. Experimental densities (ρ) with the mole fraction of ionic liquid (x_{IL}) for the binary mixtures composed of water, ethanol, or propan-1-ol with [Ch][Ala] at T = 293.15, 298.15, and 303.15 K and P = 0.1 MPa. The combined expanded uncertainties (U_c) and relative expanded uncertainties (U_r), for a level of confidence of 95 and a combined coverage factor of 1.96,[40] are $U_r(\rho)$ = 0.001 and $U_c(T)$ = 0.02 K.

[Ch][Ala] + propan-1-ol and [Ch][Ala] + ethanol. However, during most of the composition dominium, the density of [Ch][Ala] + ethanol was larger than that of [Ch][Ala] + propan-1-ol, even though pure ethanol presented a smaller density than pure propan-1-ol.

The inversion in the expected densities of [Ch][Ala] with ethanol or propan-1-ol may be explained by differences in the excess molar volumes of the binary mixtures, which translate the deviation from an ideal mixing situation. Therefore, the measured density data were used to calculate the excess molar volumes (V^E) for the studied binary mixtures, as Figure 5 illustrates, using eq 2.

$$= \ _m - \sum x_i \ _i \quad (2)$$

where V_m is the molar volume of the mixture and x_i and V_i are the mole fraction and the characteristic molar volume of component i, respectively. The molar volume of each component was calculated using eq 3.

$$V_i = \frac{i}{\rho_i} \quad (3)$$

where M_i refers to the molar mass of pure species i and ρ_i, to its measured density.

The determined excess molar volumes were all negative, as can be observed in Figure 5 and Table S3, which implies negative deviation from an ideal mixing volume, *i.e.*, larger densities than expected. Since [Ch][Ala] + ethanol had more negative excess molar volumes, *i.e.*, larger absolute excess molar volumes, than [Ch][Ala] + propan-1-ol, its verified density was larger. This fact may be explained by the dielectric constants of the solvents (at 298.15 K: 78.37 for water,[56] 23.8 for ethanol,[57] and 20.4 for propan-1-ol[58]) since larger dielectric constants imply larger polarities and easier solvation of the IL counterions. This way, for the studied systems, larger polarities of the solvent caused more negative deviations in mixture volumes and more positive deviations in the final densities. Moreover, temperature had practically no effect in the excess molar volumes of [Ch][Ala] + water, but, for the other systems, higher temperatures caused significantly more negative excess molar volumes.

The found excess molar volumes were successfully represented using a Redlich−Kister (RK)[59] expression, given by eq 4. The obtained adjustable parameters and standard deviations can be observed in Table S4.

$$V_{ij}^E \quad x_i x_j \sum_{p\ 0}^{D} \ _p \ x_i - x_j)^p \quad (4)$$

where x_i and x_j are the mole fractions of each component present in solution, B_p are the adjustable parameters, and D is the degree of the polynomial extension, which was optimized by means of a statistical test (F-test), as performed in previous works of the research group.[46,60]

One alternative (but less sensitive) way to evaluate nonideality without calculating excess molar volumes is to plot the molar volume of the mixtures with the mole fraction of the components. Since the molar volume of the mixture is directly related to the chemical potentials of the pure species,[61] a linear relation is obtained between the volume of the mixture and the mole fraction of the species for ideal mixtures. As Figure 6 shows, all the systems presented an almost ideal behavior, exhibiting very small deviations from the expected

https://doi.org/10.1021/acs.jced.3c00247
J Chem Eng Data 2024 69 338−347

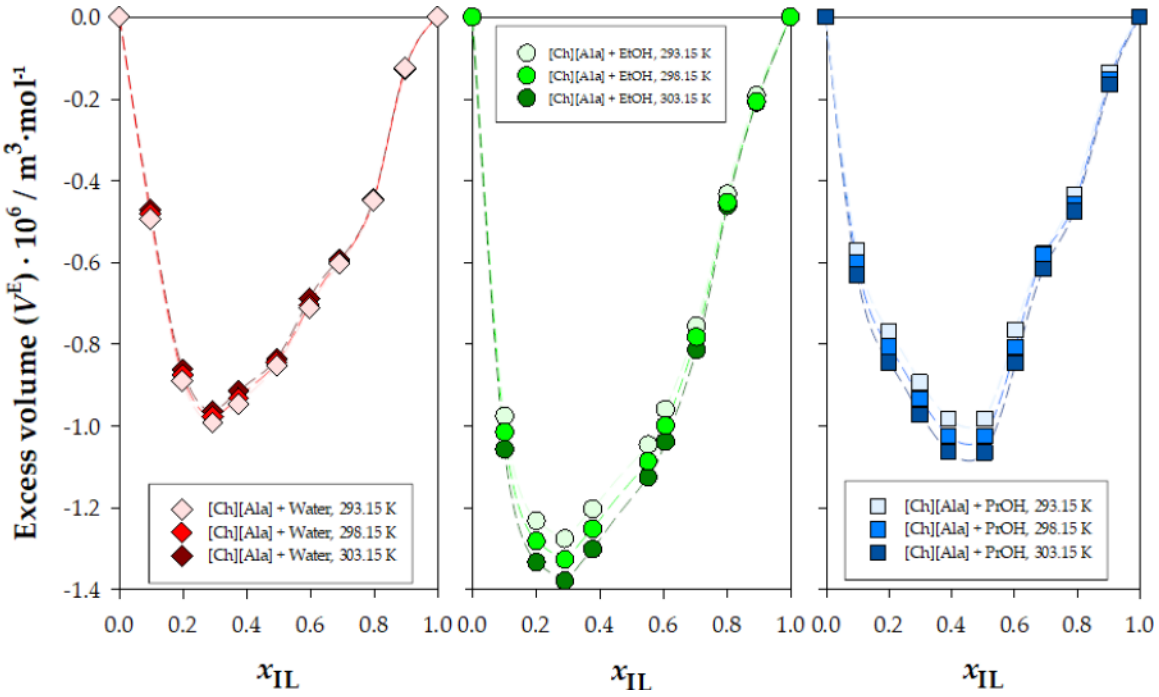

Figure 5. Excess molar volumes (V^E) with the mole fraction of ionic liquid (x_{IL}) for the binary mixtures composed of water, ethanol, or propan-1-ol with [Ch][Ala] at T = 293.15, 298.15, and 303.15 K and P = 0.1 MPa.

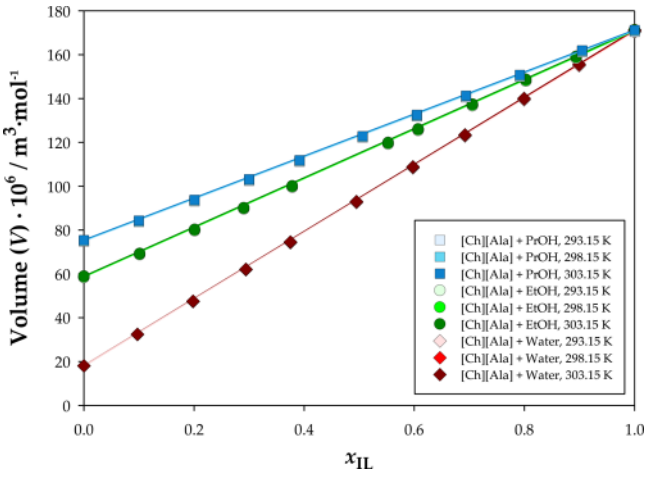

Figure 6. Molar volumes of the mixtures (V) with the mole fraction of ionic liquid (x_{IL}) for the binary mixtures composed of water, ethanol, or propan-1-ol with [Ch][Ala] at T = 293.15, 298.15, and 303.15 K and P = 0.1 MPa. Symbols represent the calculated mixture molar volumes and lines the ideal mixture molar volumes.

linear trend. This result was expected due to the small excess molar volumes (< 1.4×10^{-6} m^3·mol^{-1}) calculated by eq 2 and shown in Figure 5.

The effect of the mole fraction of [Ch][Ala] in the dynamic viscosities (η) of the binary mixtures composed of water, ethanol, or propan-1-ol can be observed in Figure 7 and Tables S5−S19. The dynamic viscosities of each studied mixture can be observed separately in Figures S6, S9, and S12. As expected, an increasing content in ionic liquid caused a growing dynamic viscosity since the viscosity at 298.15 K of pure cholinium L-alaninate (~2 Pa·s) was significantly higher than the ones of water (~8.4×10^{-4} Pa·s), ethanol (~9.0×10^{-4} Pa·s), and propan-1-ol (~1.68×10^{-3} Pa·s). Furthermore, the increase in dynamic viscosities became significantly more sensitive to growing contents of ionic liquid as it approached the composition of pure ionic liquid, which has been explained in literature by a drastic increase of the Coulomb interactions.[62] The effect of the mole fraction of ionic liquid in the shear stress and torque of the binary mixtures, at T = 288.15−308.15 K and P = 0.1 MPa, is very similar to its effect on dynamic viscosities and can be seen in Figures S7−S8, S10−S11, and S13−S14 and Tables S5−S19.

The dynamic viscosities of the mixtures which contained ethanol or propan-1-ol were found to be similar, while for the aqueous mixtures they were slightly larger, as it can be seen by the Arrhenius plots of Figure 8. These plots were obtained for the pure solvents and for the three most diluted solutions of each system using eq 5. The obtained adjustable parameters can be checked in Table S20.

$$\ln \eta) = a^{-1} \quad b \tag{5}$$

where ln(η) stands for the natural logarithm of the dynamic viscosities (Pa·s), T, for temperature, a, for the slope and b, for the y-intercept.

Dynamic viscosities of the pure solvents (water, ethanol, and propan-1-ol) were fitted as well to the Vogel−Fulcher−Tammann-Hesse (VFTH) equation, obtaining very good results, as Table 2 shows. By comparing the obtained parameters of the four components, it is clear that [Ch][Ala] has the lowest ideal glass transition temperature (T_0 = 323.3 K) while water has the highest T_0 = 609.8 K). Obviously, the values of the ideal glass transitions should not be taken as the real glass transitions of the chemical compounds and have no practical application.

Electrical conductivity (κ) measurements were also performed for the binary mixtures, as illustrated by Figure 9. Generally, [Ch][Ala] + water presented the largest conductivities, while [Ch][Ala] + propan-1-ol presented the lowest, agreeing with the solvent dielectric constants at 298.15

https://doi.org/10.1021/acs.jced.3c00247
J Chem Eng Data 2024 69 338−347

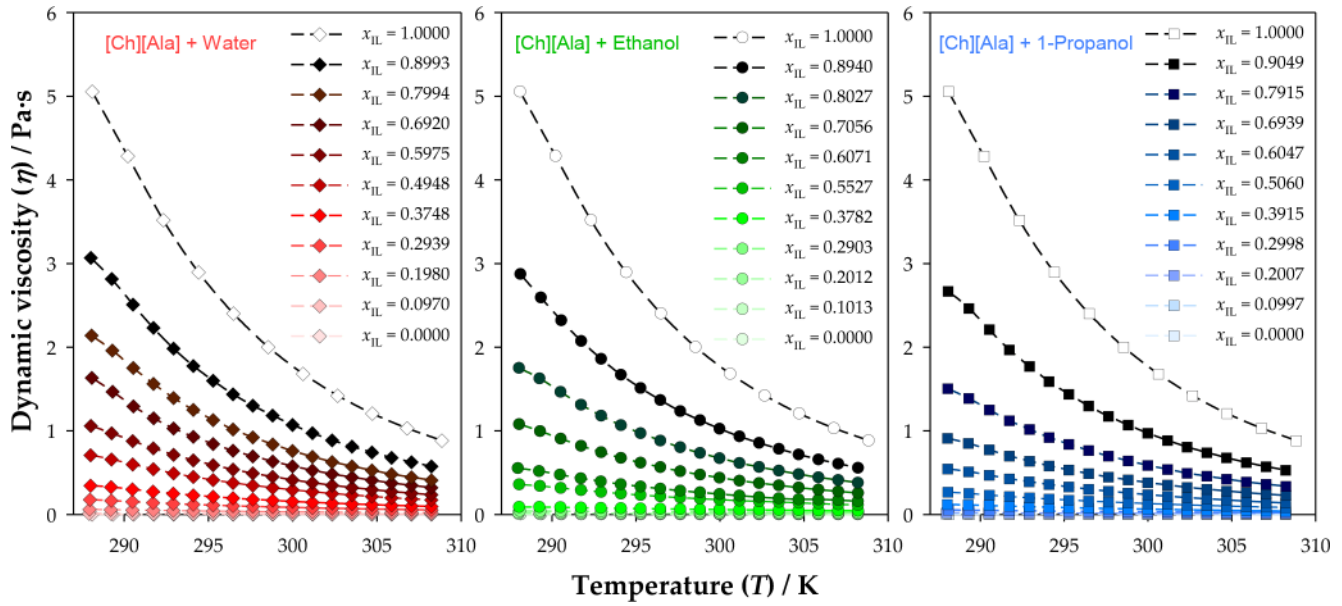

Figure 7. Experimental dynamic viscosities (η) with the mole fraction of ionic liquid (x_{IL}) for [Ch][Ala] + water (left) or ethanol (center) or propan-1-ol (right), at T = 288.15−308.15 K and P = 0.1 MPa. The combined expanded uncertainties (U_c) and relative expanded uncertainties (U_r), for a level of confidence of 95 and a combined coverage factor of 1.96,[40] are $U_r(\eta)$ = 0.24 and $U_c(T)$ = 0.02 K.

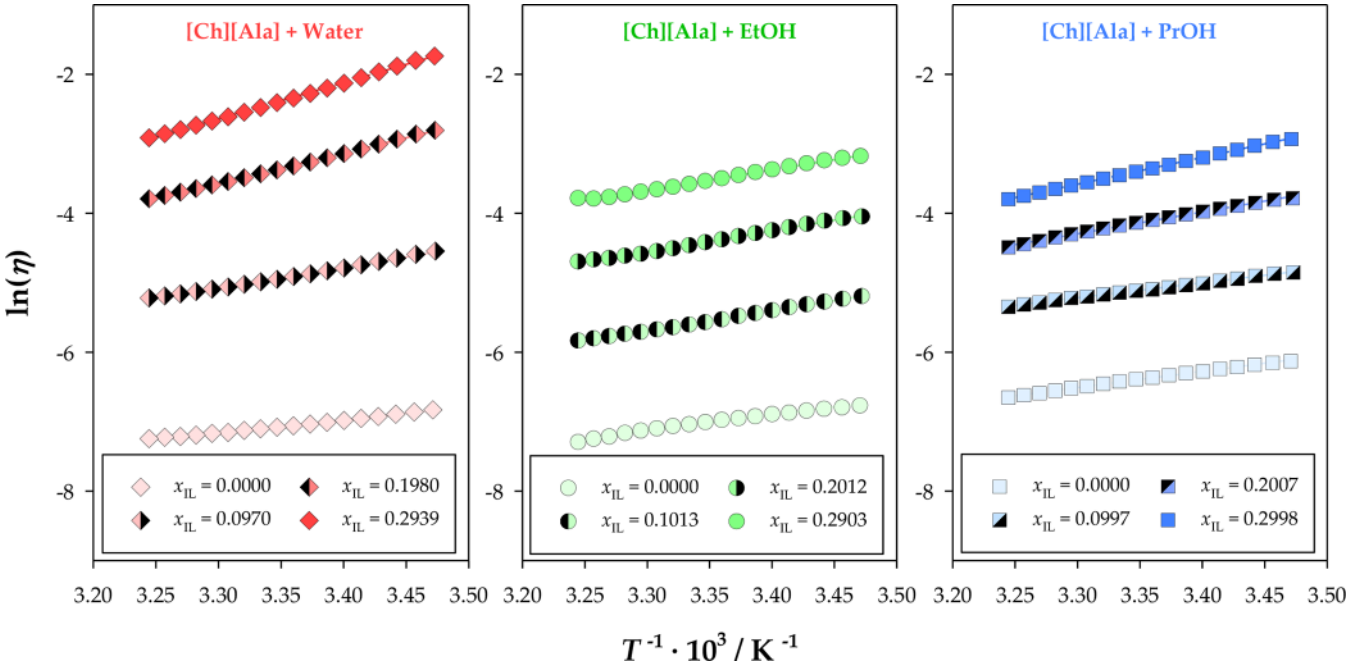

Figure 8. Arrhenius plots of the experimental dynamic viscosities for [Ch][Ala] + water (left) or ethanol (center) or propan-1-ol (right) at 0.1 MPa and $x_{IL} \approx 0$, 0.1, 0.2, and 0.3.

Table 2. Parameters of the Vogel−Fulcher−Tammann−Hesse VFTH) equation for water, ethanol, and propan-1-ol at 0.1 MPa with respective determination coefficients ^{2}), standard deviations σ_s), dynamic viscosity) range, and temperature T) range

	VFTH parameters						
solvent	$A \times 10^3$ / Pa·s	B / K	T_0 / K	R^2	$\sigma_s \times 10^3$ / Pa·s	$\eta \times 10^3$ / Pa·s	T / K
water	600.5	2040	609.8	0.9890	0.012	0.71366−1.0819	288.15−308.15
ethanol	4.693	105.8	363.1	0.9995	0.003	0.67869−1.1472	288.15−308.15
propan-1-ol	198.6	863.3	479.7	0.9998	0.004	1.2925−2.1857	288.15−308.15

K (78.37 for water,[56] 23.8 for ethanol,[57] and 20.4 for propan-1-ol[58]). As it is well-known, dielectric constants are closely related to the polarity of the chemical species, for which compounds with larger dielectric constants possess larger

https://doi.org/10.1021/acs.jced.3c00247
J Chem Eng Data 2024 69 338−347

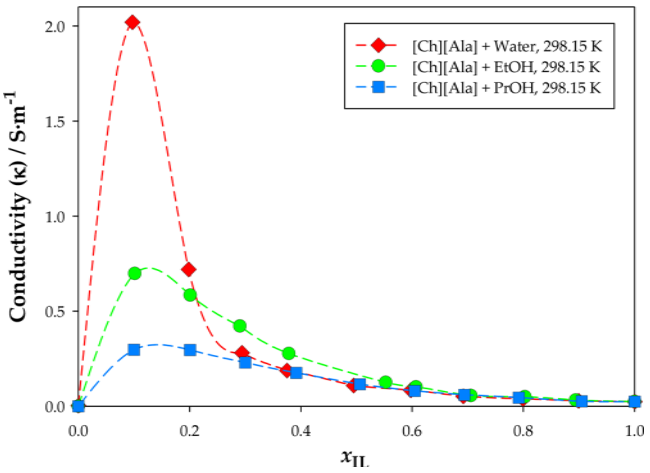

Figure 9. Experimental electrical conductivities (κ) with the mole fraction of ionic liquid (x_{IL}) for the binary mixtures composed of water, ethanol, or propan-1-ol with [Ch][Ala], at T = 298.15 K and P = 0.1 MPa. The combined expanded uncertainties (U_c) and relative expanded uncertainties (U_r), for a level of confidence of 95 and a combined coverage factor of 1.96,[40] are $U_r(\kappa)$ = 0.02 and $U_c(T)$ = 0.02 K.

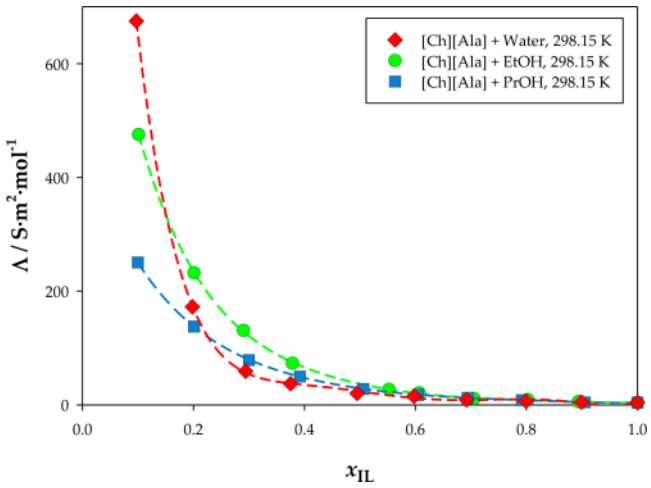

Figure 10. Calculated molar electrical conductivities (Λ) with the mole fraction of ionic liquid (x_{IL}) for the binary mixtures composed of water, ethanol, or propan-1-ol with [Ch][Ala], at T = 298.15 K and P = 0.1 MPa.

polarities, which were found to ease the dissociation of ionic liquids.[63,64] Therefore, large solvent polarities favor the dissociation of ionic liquids into their counterions (in this case, cholinium cation and L-alaninate anion), increasing the bulk electrical conductivity and explaining the differences shown by Figure 9. Moreover, all systems presented a maximum in electrical conductivity at low concentrations of ionic liquid, which has been previously described in the literature for other systems containing ionic liquids.[65,66] In this concentration zone, characterized by the presence of the referred maxima, the viscosity of the mixtures is relatively low, so the mobility of charge carriers is high, increasing electrical conductivity.[66] At even lower mole fractions of ionic liquid, the concentration of charge carriers is significantly lower and the aggregation of the ionic liquid becomes more relevant, decreasing electrical conductivity,[66,67] as can be observed in Table S21.

The system [Ch][Ala] + ethanol presented a larger conductivity than [Ch][Ala] + water in the range of 0.2 < x_{IL} < 0.6, which seems to contradict the expected trend, but this phenomenon has been reported in the literature before.[68] To enlighten this matter, the molar electrical conductivities (Λ) were calculated using eq 6,[68] as Figure 10 shows, and a persistent decrease of conductivity with increasing mole fraction of ionic liquid was observed for all systems. However, this decay was significantly more abrupt (larger absolute slope) for [Ch][Ala] + water than for the alcohol-containing systems in 0.2 < x_{IL} < 0.6, especially when compared to ethanol, which might explain [Ch][Ala] + water having a smaller conductivity than [Ch][Ala] + ethanol in that range. Some recent works on molecular dynamics simulations[69,70] have shown that water tends to create large clusters in IL−water mixtures, forming networks which connect a significant fraction of the water molecules present and allow larger electrical conductivities, while alcohols are dispersed in small clusters of dimers.[68] Therefore, the observed gap between the electric conductivities of [Ch][Ala] + water and [Ch][Ala] + alcohols in Figures 9 and 10 is probably due to the rapid size decrease of solvent clusters with growing content of ionic liquid, which is almost insignificant for alcohols (from dimers to isolated molecules) but paramount to water.

$$\Lambda \quad \kappa \tag{6}$$

where Λ is the molar electric conductivity, κ is the electric conductivity (S·m^{-1}), and c is concentration (mol·m^{-3}).

To determine the degree of dissociation (or ionicity) of pure cholinium L-alaninate, a Walden plot was created, as Figure 11 illustrates. This graphical method estimates the degree of dissociation by comparing the linearization of molar electrical conductivities and dynamic viscosities with the one obtained for a reference solution (0.01 M aqueous solution of potassium chloride, KCl).[64,66] It is based on Walden's rule, which states that the product of the equivalent conductivity and the viscosity of a solvent for a specific electrolyte is constant at a given temperature and calculates the degree of dissociation of ionic liquids ( ) using eq 7.[64] Since conductivity measurements were only performed at 298.15 K and 0.1 MPa, solely one point was obtained, presenting a degree of dissociation of 0.21 (or 21) for pure ionic liquid. This point is in the lower

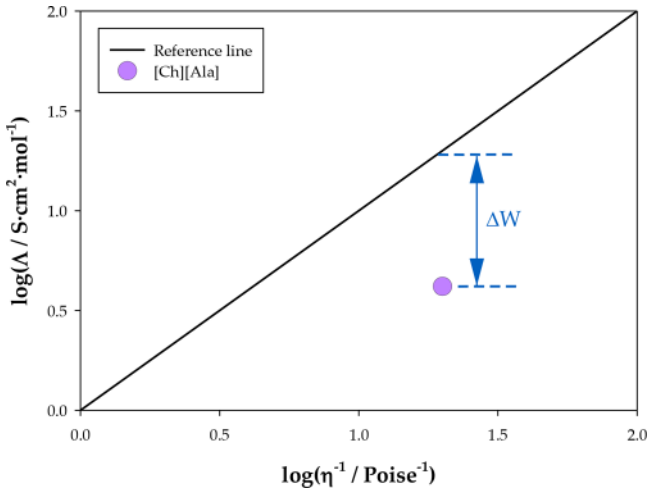

Figure 11. Walden plot for pure cholinium L-alaninate ([Ch][Ala]) at T = 298.15 K and P = 0.1 MPa.

https://doi.org/10.1021/acs.jced.3c00247
J Chem Eng Data 2024 69 338−347

part of the Walden plot, close to the reference line, so cholinium L-alaninate was considered a relatively "good" ionic liquid, meaning that its ions are evenly surrounded by a shell of counterions[71] and that low vapor pressures are expected, contributing to the eco-friendly character of this solvent.[71]

$$\alpha \quad 1^{-\Delta} \tag{7}$$

where refers to the degree of dissociation of the ionic liquid and ΔW to the vertical distance from the point of the Walden plot to the reference line.

4. CONCLUSIONS

Choline amino acid ionic liquids (CAAILs or ChAA-ILs) are a novel class of green ionic liquids, which combine large solvent power and property tunability with enhanced biodegradability and lower toxicity. These properties are considered very promising for extractive processes concerning biomolecules, such as antioxidants and vitamins, for the pharmaceutical and cosmetic industries. Nevertheless, proper thermophysical characterization of these solvents is required for the validation of thermodynamic models and for a successful industrial process design.

In this work, cholinium L-alaninate ([Ch][Ala]) was synthesized based on choline chloride and L-alanine. Its thermophysical properties (density, refractive index, and dynamic viscosity), together with its infrared (IR) transmittance spectrum and ultraviolet−visible (UV−vis) absorbance, were measured at different temperatures and 0.1 MPa. Moreover, density, electrical conductivity, and dynamic viscosity of binary mixtures containing [Ch][Ala] and water, ethanol, or propan-1-ol were assessed at different temperatures and mole fractions of ionic liquid. The obtained data were then successfully expressed using common correlation approaches: the Vogel−Fulcher−Tammann−Hesse (VFTH) equation for dynamic viscosities and the Redlich−Kister (RK) equation for excess molar volumes (which were calculated based on the density measurements). Finally, the dissociation degree (or ionicity) of pure [Ch][Ala] was estimated as 0.21 using the Walden plot methodology.

■ ASSOCIATED CONTENT

Supporting Information

The Supporting Information is available free of charge at https://pubs.acs.org/doi/10.1021/acs.jced.3c00247.

Comparison of the experimental densities, refractive indices, and dynamic viscosities with data from literature for water, ethanol, and propan-1-ol at 0.1 MPa; IR transmittance spectrum and UV−vis absorbance spectrum of [Ch][Ala]; density and refractive index of [Ch][Ala] with temperature; density and respective calculated excess molar volumes, electrical conductivity, dynamic viscosity, shear stress, and torque for the binary mixtures of [Ch][Ala] with water, ethanol, or propan-1-ol with temperature and mole fraction of ionic liquid; obtained adjustable parameters of the Redlich−Kister (RK) and Arrhenius equations (PDF).

■ AUTHOR INFORMATION

Corresponding Author

Eugénia A Macedo − *LSRE-LCM - Laboratory of Separation and Reaction Engineering − Laboratory of Catalysis and Materials Faculty of Engineering University of Porto 4200-465 Porto Portugal; ALiCE - Associate Laboratory in Chemical Engineering Faculty of Engineering University of Porto 4200-465 Porto Portugal;* orcid.org/0000-0002-0724-5380; Phone: +351 220 411 653; Email: eamacedo@fe.up.pt

Authors

Pedro Velho − *LSRE-LCM - Laboratory of Separation and Reaction Engineering − Laboratory of Catalysis and Materials Faculty of Engineering University of Porto 4200-465 Porto Portugal; ALiCE - Associate Laboratory in Chemical Engineering Faculty of Engineering University of Porto 4200-465 Porto Portugal;* orcid.org/0000-0003-4802-7301

Berta N Estevinho − *LEPABE - Laboratory for Process Engineering Environment Biotechnology and Energy Department of Chemical Engineering Faculty of Engineering and ALiCE - Associate Laboratory in Chemical Engineering Faculty of Engineering University of Porto 4200-465 Porto Portugal;* orcid.org/0000-0002-1564-6010

Complete contact information is available at: https://pubs.acs.org/10.1021/acs.jced.3c00247

Notes

The authors declare no competing financial interest.

■ ACKNOWLEDGMENTS

This work was supported by ALiCE [LA/P/0045/2020], LSRE-LCM [UIDB/50020/2020 and UIDP/50020/2020], and LEPABE [UIDB/00511/2020 and UIDP/00511/2020], funded by national funds through FCT/MCTES (PIDDAC). The authors thank Professor Margarida Bastos for all the help concerning IR transmittance measurements. P.V. is grateful for the funding support from FCT [2021.06626.BD]. B.N.E. acknowledges FCT for the contract based on the "Lei do Emprego Científico" (DL 57/2016).

■ REFERENCES

(1) Domanska, U.; Zołek-Tryznowska, Z.; Królikowski, M. Thermodynamic Phase Behavior of Ionic Liquids. *J. Chem. Eng. Data* **2007**, *52*, 1872−1880.

(2) Gómez, E.; Velho, P.; Domínguez, A.; Macedo, E. A. Thermal Analysis of Binary Mixtures of Imidazolium, Pyridinium, Pyrrolidinium, and Piperidinium Ionic Liquids. *Molecules* **2021**, *26*, 6383.

(3) Almeida, H. F. D.; Marrucho, I. M.; Freire, M. G. Removal of Nonsteroidal Anti-Inflammatory Drugs from Aqueous Environments with Reusable Ionic-Liquid-Based Systems. *ACS Sustainable Chem. Eng.* **2017**, *5*, 2428−2436.

(4) Priyanka, V. P.; Gardas, R. L. Mono- and di- cationic ionic liquids based aqueous biphasic systems for the extraction of diclofenac sodium. *Sep. Purif. Technol.* **2020**, *234*, 116048.

(5) Abouelela, A. R.; Tan, S.; Kelsall, G. H.; Hallett, J. P. Toward a Circular Economy: Decontamination and Valorization of Postconsumer Waste Wood Using the ionoSolv Process. *ACS Sustainable Chem. Eng.* **2020**, *8*, 14441−14461.

(6) Cao, C.; Xu, X.; Wang, G.; Yang, Z.; Cheng, Z.; Zhang, S.; Li, T.; Pu, Y.; Lv, G.; Xu, C.; Cai, J.; Zhou, W.; Li, F.; Pu, Z.; Li, X. Characterization of ionic liquids removing heavy metals from electroplating sludge: Influencing factors, optimization strategies and reaction mechanisms. *Chemosphere* **2023**, *324*, 138309.

(7) Lin, Z.; Su, Y.; Dai, R.; Liu, G.; Yang, J.; Sheng, W.; Zhong, Y.; Tan, L.; Chen, Y. Ionic Liquid-Induced Ostwald Ripening Effect for Efficient and Stable Tin-Based Perovskite Solar Cells. *ACS Appl. Mater. Interfaces* **2021**, *13*, 15420−15428.

(8) Sakaebe, H.; Matsumoto, H.; Tatsumi, K. Application of room temperature ionic liquids to Li batteries. *Electrochim. Acta* **2007**, *53*, 1048−1054.
(9) Stocker, M. W.; Healy, A. M.; Ferguson, S. Spray Encapsulation as a Formulation Strategy for Drug-Based Room Temperature Ionic Liquids: Exploiting Drug-Polymer Immiscibility to Enable Processing for Solid Dosage Forms. *Mol. Pharmaceutics* **2020**, *17*, 3412−3424.
(10) Stockera, M. W.; Tsolaki, E.; Harding, M. J.; Healy, A. M.; Ferguson, S. Combining Isolation-Free and Co-Processing Manufacturing Approaches to Access Room Temperature Ionic Liquid Forms of APIs. *J. Pharm. Sci.* **2023**, *112*, 2079.
(11) Handa, M.; Almalki, W. H.; Shukla, R.; Afzal, O.; Altamimi, A. S. A.; Beg, S.; Rahman, M. Active pharmaceutical ingredients (APIs) in ionic liquids: An effective approach for API physiochemical parameter optimization. *Drug Discovery Today* **2022**, *27*, 2415−2424.
(12) Tsolaki, E.; Stocker, M. W.; Healy, A. M.; Ferguson, S. Formulation of ionic liquid APIs via spray drying processes to enable conversion into single and two-phase solid forms. *Int. J. Pharm.* **2021**, *603*, 120669.
(13) Chen, S.; Zhao, Y.; Zhang, H.; Xu, P.; Jiang, Z.; Zhang, H.; Yang, J. Direct microencapsulation of Ionic-Liquid-Based shear thickening fluid via rheological behavior transition for functional applications. *Chem. Eng. J.* **2023**, *455*, 140819.
(14) Morikawa, M.; Takano, A.; Tao, S.; Kimizuka, N. Biopolymer-Encapsulated Protein Microcapsules Spontaneously Formed at the Ionic Liquid-Water Interface. *Biomacromolecules* **2012**, *13*, 4075−4080.
(15) Berton, P.; Shamshina, J. L.; Bica, K.; Rogers, R. D. Ionic Liquids as Fragrance Precursors: Smart Delivery Systems for Volatile Compounds. *Ind. Eng. Chem. Res.* **2018**, *57*, 16069−16076.
(16) Bandeira, P.; Monteiro, J.; Baptista, A. M.; Magalhaes, F. D. Tribological Performance of PTFE-based Coating Modified with Microencapsulated [HMIM][NTf2] Ionic Liquid. *Tribol Lett.* **2015**, *59*, 13.
(17) Gadilohar, B. L.; Shankarling, G. S. Choline based ionic liquids and their applications in organic transformation. *J. Mol. Liq.* **2017**, *227*, 234−261.
(18) Moriel, P.; García-Suárez, E. J.; Martínez, M.; García, A. B.; Montes-Morán, M. A.; Calvino-Casilda, V.; Banares, M. A. Synthesis, characterization, and catalytic activity of ionic liquids based on biosources. *Tetrahedron Lett.* **2010**, *51*, 4877−4881.
(19) Requejo, P. F.; Gómez, E.; Macedo, E. A. Partitioning of DNP-Amino Acids in New Biodegradable Choline Amino Acid/Ionic Liquid-Based Aqueous Two-Phase Systems. *J. Chem. Eng. Data* **2019**, *64*, 4733−4770.
(20) del Olmo, L.; Lage-Estebanez, I.; Lopez, R.; Garcia de la Vega, J. M. Understanding the Structure and Properties of Cholinium Amino Acid Based Ionic Liquids. *J. Phys. Chem. B* **2016**, *120*, 10327−10335.
(21) Miao, S.; Atkin, R.; Warr, G. Design and applications of biocompatible choline amino acid ionic liquids. *Green Chem.* **2022**, *24*, 7281−7304.
(22) Shekaari, H.; Mokhtarpour, M.; Nesari, P.; Khorsandi, M.; Behboudi, M. R.; Golmohammadi, B. Measurement and Thermodynamic Modeling of Lamotrigine Solubility in the Presence of Some Choline-Based Ionic Liquids. *J. Chem. Eng. Data* **2021**, *66*, 2200−2208.
(23) Reschke, T.; Zherikova, K. V.; Verevkin, S. P.; Held, C. Benzoic Acid and Chlorobenzoic Acids: Thermodynamic Study of the Pure Compounds and Binary Mixtures With Water. *J. Pharm. Sci.* **2016**, *105*, 1050−1058.
(24) Song, C. P.; Ramanan, R. N.; Vijayaraghavan, R.; MacFarlane, D. R.; Chan, E.-S.; Ooi, C.-W. Green, Aqueous Two-Phase Systems Based on Cholinium Aminoate Ionic Liquids with Tunable Hydrophobicity and Charge Density. *ACS Sustainable Chem. Eng.* **2015**, *3*, 3291−3298.
(25) Morandeira, L.; Sanromán, M.A.; Deive, F. J.; Rodríguez, A. Cholinium dipeptide as the cornerstone to build promising separation processes: A simultaneous recovery strategy for microalgae biorefineries. *Sep. Purif. Technol.* **2020**, *250*, 117288.
(26) Gómez, E.; Requejo, P. F.; Tojo, E.; Macedo, E. A. Recovery of flavonoids using novel biodegradable choline amino acids ionic liquids based ATPS. *Fluid Phase Equilib.* **2019**, *493*, 1−9.
(27) Morandeira, L.; Martínez-Baltasar, A.; Sanromán, M.A.; Rodríguez, A.; Deive, F. J. Designing novel biocompatible oligopeptide-based ionic liquids for greener downstream processes. *J. Cleaner Prod.* **2021**, *279*, 123356.
(28) Sun, N.; Parthasarathi, R.; Socha, A. M.; Shi, J.; Zhang, S.; Stavila, V.; Sale, K. L.; Simmons, B. A.; Singh, S. Understanding pretreatment efficacy of four cholinium and imidazolium ionic liquids by chemistry and computation. *Green Chem.* **2014**, *16*, 2546−2557.
(29) Yang, Z.-Z.; Zhao, Y.-N.; He, L.-N. CO2 chemistry: task-specific ionic liquids for CO2 capture/activation and subsequent conversion. *RSC Adv.* **2011**, *1*, 545−567.
(30) Das, S.; Karmakar, T.; Balasubramanian, S. Molecular Mechanism behind Solvent Concentration-Dependent Optimal Activity of Thermomyces lanuginosus Lipase in a Biocompatible Ionic Liquid: Interfacial Activation through Arginine Switch. *J. Phys. Chem. B* **2016**, *120*, 11720−11732.
(31) Gildseth, W.; Habenschuss, A.; Spedding, F. H. Precision measurements of densities and thermal dilation of water between 5.deg. and 80.deg. *J. Chem. Eng. Data* **1972**, *17*, 402−409.
(32) Hales, J. L.; Ellender, J. H. Liquid densities from 293 to 490 K of nine aliphatic alcohols. *J. Chem. Thermodyn.* **1976**, *8*, 1177−1184.
(33) Dávila, M. J.; Alcalde, R.; Atilhan, M.; Aparicio, S. PρT measurements and derived properties of liquid 1-alkanols. *J. Chem. Thermodyn.* **2012**, *47*, 241−259.
(34) Taib, M. M.; Murugesan, T. Density, Refractive Index, and Excess Properties of 1-Butyl-3-methylimidazolium Tetrafluoroborate with Water and Monoethanolamine. *J. Chem. Eng. Data* **2012**, *57*, 120−126.
(35) Castro, M. C.; Rodríguez, H.; Arce, A.; Soto, A. Mixtures of Ethanol and the Ionic Liquid 1-Ethyl-3-methylimidazolium Acetate for the Fractionated Solubility of Biopolymers of Lignocellulosic Biomass. *Ind. Eng. Chem. Res.* **2014**, *53*, 11850−11861.
(36) García-Abarrio, S. M.; Torcal, M.; Haya, M. L.; Urieta, J. S.; Mainar, A. M. Thermophysical properties of {(±)-linalool + propan-1-ol}: A first stage towards the development of a green process. *J. Chem. Thermodyn.* **2011**, *43*, 527−536.
(37) Huber, M. L.; Perkins, R. A.; Laesecke, A.; Friend, D. G.; Sengers, J. V.; Assael, M. J.; Metaxa, I. N.; Vogel, E.; Mares, R.; Miyagawa, K. New International Formulation for the Viscosity of H2O. *J. Phys. Chem. Ref. Data* **2009**, *38*, 101−125.
(38) Baylaucq, A.; Watson, G.; Zéberg-Mikkelsen, C.; Bazile, J.-P.; Boned, C. Dynamic Viscosity of the Binary System 1-Propanol + Toluene as a Function of Temperature and Pressure. *J. Chem. Eng. Data* **2009**, *54*, 2715−2721.
(39) De Santis, S.; Masci, G.; Casciotta, F.; Caminiti, R.; Scarpellini, E.; Campetella, M.; Gontrani, L. Cholinium-amino acid based ionic liquids: a new method of synthesis and physico-chemical characterization. *Phys. Chem. Chem. Phys.* **2015**, *17*, 20687.
(40) Chirico, R. D.; Frenkel, M.; Diky, V. V.; Marsh, K. N.; Wilhoit, R. C. ThermoMLAn XML-Based Approach for Storage and Exchange of Experimental and Critically Evaluated Thermophysical and Thermochemical Property Data. 2. Uncertainties. *J. Chem. Eng. Data* **2003**, *48*, 1344−1359.
(41) Foulet, A.; Ghanem, O. B.; El-Harbawi, M.; Léveque, J.-M.; Mutalib, M. I. A.; Yin, C.-Y. Understanding the physical properties, toxicities and anti-microbial activities of choline-amino acid-based salts: Low-toxic variants of ionic liquids. *J. Mol. Liq.* **2016**, *221*, 133−138.
(42) Li, Q.; Liu, W.; Zhu, X. Green choline amino acid ionic liquids aqueous two-phase extraction coupled with synchronous fluorescence spectroscopy for analysis naphthalene and pyrene in water samples. *Talanta* **2020**, *219*, 121305.
(43) Tao, D.-J.; Cheng, Z.; Chen, F.-F.; Li, Z.-M.; Hu, N.; Chen, X.-S. Synthesis and Thermophysical Properties of Biocompatible

Cholinium-Based Amino Acid Ionic Liquids. *J. Chem. Eng. Data* **2013**, *58*, 1542−1548.
(44) Liu, Q.-P.; Hou, X.-D.; Li, N.; Zong, M.-H. Ionic liquids from renewable biomaterials: synthesis, characterization and application in the pretreatment of biomass. *Green Chem.* **2012**, *14*, 304−307.
(45) Le Donne, A.; Bodo, E. Cholinium amino acid-based ionic liquids. *Biophys. Rev.* **2021**, *13*, 147−160.
(46) Requejo, P. F.; González, E. J.; Macedo, E. A.; Domínguez, A. Effect of the temperature on the physical properties of the pure ionic liquid 1-ethyl-3-methylimidazolium methylsulfate and characterization of its binary mixtures with alcohols. *J. Chem. Thermodyn.* **2014**, *74*, 193−200.
(47) González, E. J.; González, B.; Macedo, E. A. Effect of the relative humidity and isomeric structure on the physical properties of pyridinium based-ionic liquids. *J. Chem. Thermodyn.* **2015**, *86*, 96−105.
(48) Vogel, H. Das Temperaturabhaengigkeitsgesetz der Viskositaet von Fluessigkeiten. *Phys. Z.* **1921**, *22*, 645.
(49) Fulcher, G. S. Analysis of Recent Measurements of the Viscosity of Glasses. *J. Am. Ceram. Soc.* **1925**, *8*, 339−355.
(50) Tammann, G.; Hesse, W. Die Abhangigkeit der Viscositat von der Temperatur bie unterkuhlten Flussigkeiten. *Z. anorg. allg.* **1926**, *156*, 245−257.
(51) Nascimento, M. L. F.; Aparicio, C. Data classification with the Vogel-Fulcher-Tammann-Hesse viscosity equation using correspondence analysis. *Phys. B* **2007**, *398*, 71−77.
(52) Mano, J. F.; Pereira, E. Data Analysis with the Vogel-Fulcher-Tammann-Hesse Equation. *J. Phys. Chem. A* **2004**, *108*, 10824−10833.
(53) Rodríguez, H.; Brennecke, J. F. Temperature and Composition Dependence of the Density and Viscosity of Binary Mixtures of Water + Ionic Liquid. *J. Chem. Eng. Data* **2006**, *51*, 2145−2155.
(54) Cohen, M. H.; Turnbull, D. Molecular Transport in Liquids and Glasses. *J. Chem. Phys.* **1959**, *31*, 1164−1169.
(55) Adam, G.; Gibbs, J. H. On the temperature dependence of cooperative relaxation properties in glass-forming liquids. *J. Chem. Phys.* **1965**, *43*, 139−146.
(56) Vidulich, G. A.; Kay, R. L. The dielectric constant of water between 0° and 40°. *J. Phys. Chem.* **1962**, *66*, 383.
(57) Celiano, A. V.; Gentile, P. S.; Cefola, M. Dielectric Constants of Binary Systems. *J. Chem. Eng. Data* **1962**, *7*, 391.
(58) Gover, T. A.; Sears, P. G. Conductances of Some Electrolytes in 1-Propanol at 25°. *J. Phys. Chem.* **1956**, *60*, 330−332.
(59) Redlich, O.; Kister, A. T. Algebraic Representation of Thermodynamic Properties and the Classification of Solutions. *Ind. Eng. Chem.* **1948**, *40*, 345−348.
(60) González, E. J.; González, B.; Macedo, E. A. Thermophysical Properties of the Pure Ionic Liquid 1-Butyl-1-methylpyrrolidinium Dicyanamide and Its Binary Mixtures with Alcohols. *J. Chem. Eng. Data* **2013**, *58*, 1440−1448.
(61) Almeida, H. F. D.; Lopes, J. N. C.; Rebelo, L. P. N.; Coutinho, J. A. P.; Freire, M. G.; Marrucho, I. M. Densities and Viscosities of Mixtures of Two Ionic Liquids Containing a Common Cation. *J. Chem. Eng. Data* **2016**, *61*, 2828−2843.
(62) Gong, Y.; Shen, C.; Lu, Y.; Meng, H.; Li, C. Viscosity and Density Measurements for Six Binary Mixtures of Water (Methanol or Ethanol) with an Ionic Liquid ([BMIM][DMP] or [EMIM][DMP]) at Atmospheric Pressure in the Temperature Range of (293.15 to 333.15) K. *J. Chem. Eng. Data* **2012**, *57*, 33−39.
(63) Lopes, C.; Velho, P.; Macedo, E. A. Predicting the ionicity of ionic liquids in binary mixtures based on solubility data. *Fluid Phase Equilib.* **2023**, *567*, 113717.
(64) Velho, P.; Lopes, C.; Macedo, E. A. Predicting the ionicity of ionic liquids in binary mixtures based on solubility data: II. *Fluid Phase Equilib.* **2023**, *569*, 113766.
(65) Stoppa, A.; Hunger, J.; Buchner, R. Conductivities of Binary Mixtures of Ionic Liquids with Polar Solvents. *J. Chem. Eng. Data* **2009**, *54*, 472−479.
(66) García-Mardones, M.; Osorio, H. M.; Lafuente, C.; Gascón, I. Ionic Conductivities of Binary Mixtures Containing Pyridinium-Based Ionic Liquids and Alkanols. *J. Chem. Eng. Data* **2013**, *58*, 1613−1620.
(67) Zhang, Q.-G.; Sun, S.-S.; Pitula, S.; Liu, Q.-S.; Welz-Biermann, U.; Zhang, J.-J. Electrical Conductivity of Solutions of Ionic Liquids with Methanol, Ethanol, Acetonitrile, and Propylene Carbonate. *J. Chem. Eng. Data* **2011**, *56*, 4659−4664.
(68) Rilo, E.; Vila, J.; García-Garabal, S.; Varela, L. M.; Cabeza, O. Electrical Conductivity of Seven Binary Systems Containing 1-Ethyl-3-methyl Imidazolium Alkyl Sulfate Ionic Liquids with Water or Ethanol at Four Temperatures. *J. Phys. Chem. B* **2013**, *117*, 1411−1418.
(69) Méndez-Morales, T.; Carrete, J.; Cabeza, O.; Gallego, L. J.; Varela, L. M. Molecular Dynamics Simulation of the Structure and Dynamics of Water-1-Alkyl-3-methylimidazolium Ionic Liquid Mixtures. *J. Phys. Chem. B* **2011**, *115*, 6995−7008.
(70) Carrete, J.; Méndez-Morales, T.; Cabeza, O.; Lynden-Bell, R. M.; Gallego, L. J.; Varela, L. M. Investigation of the Local Structure of Mixtures of an Ionic Liquid with Polar Molecular Species through Molecular Dynamics: Cluster Formation and Angular Distributions. *J. Phys. Chem. B* **2012**, *116*, 5941−5950.
(71) Angell, C. A.; Byrne, N.; Belieres, J.-P. Parallel Developments in Aprotic and Protic Ionic Liquids: Physical Chemistry and Applications. *Acc. Chem. Res.* **2007**, *40*, 1228−1236.

https://doi.org/10.1021/acs.jced.3c00247
J Chem Eng Data 2024 69 338−347